Two-Photon Absorption in Cu_2O

K. C. Rustagi,* F. Pradere, and A. Mysyrowicz
Laboratoire d'Optique Quantique du Centre National de la Recherche Scientifique, Bâtiment 503, Université de Paris-Sud, 91405 Orsay, France
(Received 8 March 1973)

In the first part, a general theoretical treatment of two-photon absorption in semiconductors is presented. It includes excitonic effects in the intermediate as well as final states. *s* and *p* excitonic final states are discussed separately. In the second part, the two-photon absorption of Cu_2O at 77 °K is presented. The spectral region studied includes transitions from the two upper valence bands to the two lower conduction bands. Excitonic structures are observed. The results are discussed within the framework of the theory presented in part one.

I. INTRODUCTION

The study of two-photon absorption (TPA) spectra has emerged, in recent years, as a very useful tool for the investigation of solids.[1] TPA is an elementary excitation process in which two photons *simultaneously* give their energies to the medium. Quite generally, the rate of two-photon transitions depends on the polarization vectors $\hat{\epsilon}_1$ and $\hat{\epsilon}_2$ and the frequencies ω_1 and ω_2 of the two photons. Further, the selection rules for TPA are different from those for the one-photon absorption. Accordingly, a detailed study of TPA spectra in all possible independent experimental configurations provides several independent material parameters which are not available from the more conventional one-photon spectroscopy. Experimentally, one obtains TPA spectra by measuring the absorption coefficient $\alpha^{(2)}(\omega_1, \omega_2)$ of a relatively weak light beam characterized by $\hat{\epsilon}_2$, ω_2 in the presence of a strong laser beam characterized by $\hat{\epsilon}_1$, ω_1. The crystal is transparent at both the frequencies ω_1 and ω_2. Since $\alpha^{(2)}$ is directly proportional to the intensity of the laser beam, its magnitude can be controlled by adjusting the laser intensity. This permits one to measure a large variation of two-photon transition rates using the largest available single crystals. In contrast, the only way of measuring one-photon absorption spectra in regions of strong absorption lies in using thinner and thinner samples, which are usually difficult to obtain. Further, unlike the experiments measuring reflectivity or those measuring absorption in thin samples, TPA experiments are not affected by surface properties of the sample.

In this paper we present the results of a detailed investigation of the TPA spectra of Cu_2O. This crystal displays, in one-photon spectroscopy, a rich variety of excitonic transitions.[2] As expected, excitonic states are also very important in the study of TPA spectra of Cu_2O.

Loudon[3] was the first to consider that the electron-hole pair created by a two-photon electronic transition must form an excitonic state. In his theory, the first photon is absorbed, creating a virtual electron-hole pair state. The absorption of the second photon then leads to the virtual state being scattered into the final electron-hole pair state, with either the electron or the hole making an *interband* transition. The Coulomb attraction between the hole and the electron in the final state was accounted for, but that in the intermediate state was ignored. The presence of at least three bands is essential for a calculation of this type. Loudon predicted the appearance of a strong line due to the creation of $n=1$ exciton of the yellow series of Cu_2O. In the electric-dipole approximation, this line is forbidden in the one-photon absorption. It was later shown by Mahan[4] that most of the available experimental data on other materials could be well understood on the basis of a two-band model, first proposed by Hopfield and Worlock.[5] In this calculation the system is restricted to the initial valence band and the final conduction band only. Coulomb interaction between the electron and hole in the intermediate, as well as final state, plays an important role. It is reasonable to expect the two-band contribution to be more important when the corresponding interband transition is allowed in the one-photon spectrum. In other cases, such as that considered by Loudon, the adequacy of two-band contributions may be questionable.[6] In order to compare the two contributions, one must take Coulomb attraction in the intermediate state for the three-band model also into account. With this in view, a theory of two-photon absorption in crystals is presented in Sec. II.

We find that the Coulomb effects in the intermediate state are negligible when neither of the two frequencies ω_1 and ω_2 are close to the intermediate excitonic levels. This is made more precise by defining the parameters κ_1 and κ_2 as

$$\kappa_\alpha = \left(\frac{R_i}{E_{gi} - \hbar\omega_\alpha}\right)^{1/2},$$

where $\alpha = 1, 2$, and R_i and E_{gi} are the Rydberg and

the band gap corresponding to the intermediate excitonic level. In all cases, where $\kappa_\alpha \ll 1$, except for the two-band contribution to s excitonic final states, approximate results may be obtained by neglecting Coulomb effects in the intermediate states. The two-band contribution to s excitonic final states is an exception[4] in that the neglect of Coulomb effect in the intermediate state leads to divergent results for the two-photon transition rate.

The relative importance of the two-band and three-band term depends on the band-structure parameters of the material and the frequencies ω_1 and ω_2. The two terms leading to the same final state may interfere destructively when they are comparable. With this in view the TPA leading to s excitonic final states is considered separately from that to p excitonic states.

In Sec. III we describe the experimental setup. In Sec. IV, we present our results on Cu_2O and interpret them. Apart from some preliminary results[7] from our group, no experimental results are known for Cu_2O. Finally, we present our conclusions in Sec. V.

II. THEORY

The general expression for the two-photon absorption coefficient may be derived using the standard time-dependent perturbation theory. In the electric-dipole approximation one obtains

$$\alpha^{(2)}(\omega_1,\omega_2)=\frac{(2\pi)^3e^4P_1}{m^4c^2\hbar^3\omega_1^2\omega_2 n_1 n_2}\,\rho(\omega_f)\,|A_{fi}|^2\,, \tag{2.1}$$

where P_1 is the power of the laser beam in the medium, n_1 and n_2 are the indices of refraction at ω_1 and ω_2, and $\rho(\omega_f)$ is the density of final states. The composite matrix element A_{fi} is given by

$$A_{fi}=\hbar\sum_l \frac{\langle f|\hat{\epsilon}_2\cdot\vec{P}|l\rangle\langle l|\hat{\epsilon}_1\cdot\vec{P}|i\rangle}{E_l-E_i-\hbar\omega_1} + \frac{\langle f|\hat{\epsilon}_1\cdot\vec{P}|l\rangle\langle l|\hat{\epsilon}_2\cdot\vec{P}|i\rangle}{E_l-E_i-\hbar\omega_2}\,, \tag{2.2}$$

where $\vec{P}$ denotes the total momentum operator, $|n\rangle$ denotes the electronic eigenstates, and E_n the corresponding energies. In obtaining Eqs. (2.1) and (2.2), the interaction between the medium and the electromagnetic field has been represented by the Hamiltonian

$$H'=-(e/mc)\vec{A}\cdot\vec{P}\,, \tag{2.3}$$

where $\vec{A}$ is the vector potential of the field.

Calculation of Matrix Elements

The main task in the interpretation of TPA lies in calculating A_{fi} of Eq. (2.2). For a nonmetallic crystal at low temperature, the initial or ground state consists of a set of completely filled valence bands, and, in the independent-particle model, all excited states are obtained from this by transferring an electron from the valence-band state v, $-\vec{k}_h$ to the conduction-band state c, $\vec{k}_e$. We denote such an excited state by $\Psi(c,\vec{k}_e;\,v,\vec{k}_h)$ and the ground state by Ψ_0. Further, when the Coulomb interaction between the electron and the hole is taken into account, all excited states may be described by linear combinations of the type[8]

$$\Psi_\alpha=\sum_{\vec{k}_e,\vec{k}_h} A_\alpha(\vec{k}_e,\vec{k}_h)\Psi(c\vec{k}_e;\,v\vec{k}_h)\,, \tag{2.4}$$

where α denotes a set of quantum numbers. In the effective-mass approximation, A_α is given by

$$\sum_{\vec{k}_e,\vec{k}_h} A_\alpha(\vec{k}_e,\vec{k}_h)\,e^{i\vec{k}_e\cdot\vec{r}_e+i\vec{k}_h\cdot r_h}=\sqrt{\Omega}\,\delta_{K,\vec{k}_e+\vec{k}_h}\,\phi_{\underline{n}}^{cv}(\vec{r}_e-\vec{r}_h)\,e^{i\vec{K}\cdot\vec{\rho}}\,, \tag{2.5}$$

where $\vec{\rho}$ is the center-of-mass coordinate of the electron-hole pair, Ω is the volume of the crystal, and $\phi_{\underline{n}}^{cv}$ is the normalized wave function of relative motion of the electron and hole.[9] This electron-hole system is like a hydrogen atom with the proton charge replaced by e/ϵ_s (ϵ_s is the static dielectric constant) and with the reduced mass $\mu_{cv}=m_cm_v/m_c+m_v)$, where m_c and m_v are the effective masses of the conduction and valence bands, respectively. From the foregiong discussion, it is obvious that the index α denotes collectively the band indices c and v, the total wave vector $\vec{K}$, and the set of hydrogenic quantum numbers $\underline{n}$.

In order to calculate the composite matrix element A_{fi}, we consider the case when the final state $|f\rangle$ and the intermediate state $|l\rangle$ are both excitonic states described by Eqs. (2.4) and (2.5). Our results are more general than those of earlier theoretical papers,[3,4,10] and we shall explicitly state the situations in which the results of one or the other of these would be a good approximation. Since $\vec{P}$ does not connect states with different $\vec{K}$, and since the total wave vector of the state $|i\rangle$ is zero, $|l\rangle$ and $|f\rangle$ both have $\vec{K}=0$. Then let $|l\rangle$ be an excitonic state with hydrogenic quantum numbers $\underline{n}'$, with electron in the conduction band c' and hole in the valence band v'. The final state $|f\rangle$ is similarly specified by $\underline{n}$, c, and v. In this case, the relevant matrix elements are given by

$$\langle l|\vec{P}|i\rangle=\sum_{\vec{k}_e} A^*_{\underline{n}'c'v'}(\vec{k}_e,-\vec{k}_e)\,\vec{p}_{c'v'}(\vec{k}_e) \tag{2.6}$$

and

$$\langle f|\vec{P}|l\rangle=\sum_{\vec{k}_e} A^*_{\underline{n}cv}(\vec{k}_e,-\vec{k}_e)A_{\underline{n}'c'v'}(\vec{k}_e,-\vec{k}_e) \times[-\delta_{c,c'}(1-\delta_{vv'})\vec{p}_{v',v}(\vec{k}_e)+\delta_{v,v'}(1-\delta_{cc'})\vec{p}_{cc'}(\vec{k}_e) +\delta_{cc'}\delta_{vv'}(m\hbar/\mu_{cv})\vec{k}_e]\,, \tag{2.7}$$

where $p_{bb'}(\vec{K})$ are the interband matrix elements of momentum in Bloch states. In Eq. (2.7), the first two terms in the square brackets correspond to an interband transition, while the third term depicts an intraband transition. To obtain this last term

one used the relations[11]

$$(b\vec{k}|\vec{p}|b\vec{k}) = \frac{m}{\hbar}\frac{\partial}{\partial \vec{k}}(E_{bk})$$

and

$$\sum_{\vec{k}} \frac{\partial}{\partial \vec{k}}(E_{bk}) = 0 ,$$

where the summation is over the complete zone. Following Elliott,[8] we assume that $A(\vec{k}_e, -\vec{k}_e)$ is substantially large only over a small region of $\vec{k}$ space, in which the interband matrix elements of momentum vary only slightly. It is thus a good approximation to expand

$$p^{\mu}_{cv}(\vec{k}) = p^{\mu}_{cv}(0) + k^{\nu}\left.\frac{\partial p^{\mu}_{cv}}{\partial k^{\nu}}\right|_0 + \cdots \qquad (2.8)$$

and retain only the leading terms in this expansion. Retaining only the first two terms,

$$\langle l|P^{\alpha}|i\rangle \simeq \sqrt{\Omega}\,[p^{\alpha}_{c'v'}(0)(\phi^{c'v'}_{\underline{n}'})^{*}_{0} + M^{\alpha\beta}_{c'v'}(p^{\beta}\phi^{c'v'}_{\underline{n}'})^{*}_{0}] , \qquad (2.9)$$

where ϕ is an hydrogenic function, and the subscript zero denotes that the quantity is evaluated at $\vec{r}=0$ and where we have used the definition

$$M^{\alpha\beta}_{bb'} = \left.\frac{\partial p^{\alpha}_{bb'}}{\partial \hbar k^{\beta}}\right|_0 . \qquad (2.10)$$

The matrix element Eq. (2.9) is familiar from the theory of the single-photon absorption; the two terms in Eq. (2.9) lead to the formation of s and p excitonic states, respectively. The second matrix element describing an interexcitonic transition, is similarly found to be

$$\langle f|P^{\alpha}|l\rangle = \{-\delta_{cc'}(1-\delta_{vv'})p^{\alpha}_{v'v}(0) + \delta_{vv'}(1-\delta_{cc'})p^{\alpha}_{cc'}(0)\}(\underline{n}cv|\underline{n}'c'v')$$
$$+\{-M^{\alpha\beta}_{v'v}\delta_{cc'}(1-\delta_{vv'}) + M^{\alpha\beta}_{cc'}\delta_{vv'}(1-\delta_{cc'}) + \delta_{cc'}\delta_{vv'}\delta_{\alpha\beta}[m/\mu_{cv}]\}(\underline{n}cv|p^{\beta}|\underline{n}'c'v') , \qquad (2.11)$$

where parentheses are used to denote matrix elements between hydrogenic states. The first term stands for an interexcitonic transition, accompanied by an interband transition, which is allowed at $\vec{k}=0$. The second term is obtained when the interband transition is not allowed at $\vec{k}=0$, or when the intermediate and final excitonic states belong to the same pair of bands. The matrix element for an intraband transition is like that for an interband transition, which is forbidden at $\vec{k}=0$. In fact, the definition of $M_{bb'}$ could be generalized to include the case $b=b'$ and we may then use

$$m/\mu_{cv} = M_{cc} - M_{vv} \qquad (2.12)$$

in the second term in Eq. (2.11).

It is interesting here to consider the order of magnitude of the parameter M_{cv}. Using $\vec{k}\cdot\vec{p}$ perturbation theory, Elliott[8] has obtained the following expression for M_{cv}:

$$M^{\mu\nu}_{cv} = \frac{1}{m\hbar}\sum_i{}'\left(\frac{p^{\nu}_{ci}p^{\mu}_{iv}}{\omega_{ci}} + \frac{p^{\mu}_{ci}p^{\nu}_{iv}}{\omega_{vi}}\right) , \qquad (2.13)$$

where the prime on the summation denotes that terms with vanishing denominators are omitted.

Comparing this with the f sum rule,

$$\frac{1}{\hbar^2}\frac{\partial^2 E_{ck}}{\partial k_{\mu}\partial k_{\nu}} = \frac{1}{m^2}\sum_i{}'\frac{p^{\mu}_{ci}p^{\nu}_{ic} + p^{\nu}_{ci}p^{\mu}_{ic}}{\hbar\omega_{ci}} + \frac{1}{m}\delta_{\mu\nu} , \qquad (2.14)$$

one may expect that M_{cv} should be on the order of (m/μ_{cv}). Note, however, that unlike the f sum rule, only those intermediate states contribute to M_{cv}, which are connected to both the bands c and v. Due to this, M_{cv} may sometimes be considerably different from (m/μ_{cv}) and should be considered an important additional parameter of the band structure of the solid.[12] Combining the results of Eqs. (2.9) and (2.11), we find

$$A_{fi}(\omega_1,\omega_2) = \sqrt{\Omega}\left(-\sum_{\underline{n}'}\sum_{v'\neq v}\{\hat{\epsilon}_1\cdot\vec{p}_{v'v}(0)(\underline{n}cv|\underline{n}'cv') + \hat{\epsilon}_1\cdot M_{v'v}\cdot(\underline{n}cv|\vec{p}|\underline{n}'cv')\}\right.$$
$$\times\{\hat{\epsilon}_2\cdot\vec{p}_{cv'}(0)(\phi^{cv'}_{\underline{n}'})^{*}_{0} + \hat{\epsilon}_2\cdot M_{cv'}\cdot(\vec{p}\phi^{cv'}_{\underline{n}'})^{*}_{0}\}/(\omega_{\underline{n}'cv'} - \omega_2)$$
$$+\sum_{n'}\sum_{c'\neq c}\{\hat{\epsilon}_1\cdot\vec{p}_{cc'}(0)(\underline{n}cv|\underline{n}'c'v) + \hat{\epsilon}_1\cdot M_{cc'}\cdot(\underline{n}cv|\vec{p}|\underline{n}'c'v)\}$$
$$\times\{\vec{\epsilon}_2\cdot\vec{p}_{c'v}(0)(\phi^{c'v}_{\underline{n}'})^{*}_{0} + \vec{\epsilon}_2\cdot M_{c'v}\cdot(\vec{p}\phi^{c'v}_{\underline{n}'})^{*}_{0}\}/(\omega_{\underline{n}'c'v} - \omega_2)$$
$$+\frac{m}{\mu_{cv}}\sum_{\underline{n}'}{}'\frac{(ncv|\hat{\epsilon}_1\cdot\vec{p}|n'cv)}{(\omega_{\underline{n}'cv} - \omega_2)}\{\hat{\epsilon}_2\cdot\vec{p}_{cv}(0)(\phi^{cv}_{\underline{n}'})^{*}_{0} + \hat{\epsilon}_2\cdot M_{cv}\cdot(\vec{p}\phi^{cv}_{\underline{n}'})^{*}_{0}\}$$
$$\left.+(\hat{\epsilon}_1,\omega_1\leftrightarrow\hat{\epsilon}_2,\omega_2)\right) . \qquad (2.15)$$

At this stage, the calculation divides itself into two parts: (a) the summation over $\underline{n}'$, the hydrogenic index of the intermediate excitonic state, and (b) the summation over the band indices c' and v'. The first summation here is a direct result of including the Coulomb attraction between the electron and hole in the intermediate state. This can be reduced to an integral which can be evaluated by a simple computer program. The second summation is more difficult. Except in some limiting cases, one is obliged to restrict this summation to a few terms; which conduction or valence bands contribute most significantly as the intermediate state depends on the material and the frequencies ω_1 and ω_2. A reasonable judgment can usually be made by a careful analysis of the linear optical properties and the symmetry of the wave functions. A partial solution of the problem is obtained by neglecting all the three-band terms [first two terms in Eq. (2.15)]. In this approximation, Mahan[4] found fair agreement with the experimental data on alkali halides. On the other hand, Loudon's calculation[3] can be considered as an approximate evaluation of the three-band terms. If, following Loudon, one neglects the $\vec{k}$ dependence of all interband momentum matrix elements, i.e., puts all $M_{bb'}=0$, $b\neq b'$, the three-band terms give rise to s excitonic final states only. In centrosymmetric crystals, this contribution occurs only when the final conduction and valence bands have the same parity at $\vec{k}=0$. The next-higher-order terms, introduced due to the $\vec{k}$ dependence of interband momentum matrix elements, are of order $(\hbar/ap_{bb'})$ compared to these, and contribute to p excitonic final states,[13] where a denotes the exciton radius. Similarly, as shown by Mahan, the lowest-order (in the $\vec{k}$ dependence of p_{cv}) two-band term contributes only to p excitonic states: The two-band contribution to s excitonic final states is smaller by a factor $\hbar M_{cv}/ap_{cv}$. The relative importance of the two-band and the three-band terms depends critically on the frequencies ω_1 and ω_2 and on the intermediate states involved in the latter. We shall discuss this separately for the s and p excitonic final states, respectively. The TPA by d-like final states, also described by Eq. (2.15), is not discussed in detail, since higher-order terms in the expansion (2.8) would also contribute comparably to TPA by d excitonic final states.

s Excitonic Final States

An evaluation of each three-band term giving rise to s excitonic final states involves summations of the form

$$S_{c'v'}(\omega)=\sum_{\underline{n}'}\frac{(\underline{n}cv|\underline{n}'c'v')}{\omega_{\underline{n}'c'v'}-\omega}\,(\phi_{\underline{n}'}^{c'v'})_0^* \tag{2.16}$$

with either $c'=c$ or $v'=v$. The neglect of excitonic effects in the intermediate state amounts to replacing $S_{c'v'}(\omega)$ by

$$\frac{1}{\omega_{c'v'}-\omega}\,(\phi_{\underline{n}}^{cv})_0^* . \tag{2.17}$$

At first sight, this is equivalent to neglecting the difference between the masses of the intermediate- and final-state excitons, so that due to orthogonality only the $\underline{n}'=\underline{n}$ term contributes in Eq. (2.16); and then replacing the intermediate-state exciton energy by the corresponding band gap. In general, it is difficult to justify this procedure. Therefore, we have reduced the summation (2.16) to a form which enables us to appreciate precisely the difference between Eqs. (2.16) and (2.17). We write[4]

$$\sum_{\underline{n}'}\frac{(\phi_{\underline{n}'}^{c'v'})_0^*\phi_{\underline{n}'}^{c'v'}(\vec{r})}{\omega_{\underline{n}'c'v'}-\omega}=\frac{\mu_{c'v'}\Gamma(1-\kappa)}{2\pi r\hbar}\,W_{\kappa,1/2}\!\left(\frac{2r}{a\kappa}\right), \tag{2.18}$$

where κ is defined by

$$\kappa_{c'v'}(\omega)=[R_{c'v'}/(\hbar\omega_{c'v'}-\hbar\omega)]^{1/2} . \tag{2.19}$$

In the above equations, W is Whittaker's function, $R_{c'v'}$ and $a_{c'v'}$ are the Rydberg and the radius of the intermediate-state excitons. We have omitted the indices on a and κ in Eq. (2.18) and in the following discussion. For bound final states, the summation (2.16) becomes

$$S_{c'v'}(\omega)=(2\mu_{c'v'}/\hbar)\,\Gamma(1-\kappa)\int_0^\infty dr\,r \times\phi_{\underline{n}}^{cv}(r)W_{\kappa,1/2}(2r/a\kappa) \tag{2.20}$$

after integration on the orientation of $\vec{r}$. Using Eqs. (2.11) and (2.12) of Ref. 4, and the relation

$$\frac{\partial}{\partial\rho}\,{}_1F_1(a,c,\rho)=(a/c)\,{}_1F_1(a+1,c+1,\rho) \tag{2.21}$$

for the standard hypergeometric function ${}_1F_1(a,c,\rho)$, we find

$$S_{cv'}(\omega)=(\phi_{\underline{n}}^{cv})_0^*\,\frac{I_{s,\underline{n}}[\kappa_{c'v'}(\omega)]}{(\omega_{c'v'}-\omega)} , \tag{2.22}$$

where $I_{s,n}$ is an integral given by

$$I_{s,\underline{n}}(\kappa)=\frac{1}{2}\int_0^\infty dt\left(\frac{1+t}{t}\right)^{\kappa} \times\frac{(t+\frac{1}{2}-\underline{n}/2b)\,(t+\frac{1}{2}-1/2b)^{\underline{n}-2}}{(t+\frac{1}{2}+1/2b)^{\underline{n}+2}} \tag{2.23}$$

with

$$b=\frac{a_{cv}\underline{n}}{a_{c'v'}\kappa_{c'v'}(\omega)} . \tag{2.24}$$

The integral $I_{s,\underline{n}}$ can be reduced to a double series following the methods of Ref. 4, but we do not find this useful either for computational simplification or for gaining any physical insight. For continuum states the calculations proceed along the same way. Equation (2.23) would still be valid if one replaces $I_{s,n}(\kappa)$ by

$$I_{s,k}(\kappa)=\tfrac{1}{2}\int_0^\infty dt(t+\tfrac{1}{2}-1/2b')$$

$$\times[(1+t)/t]^{\kappa}[(t+\tfrac{1}{2})^2+b'^2/4\eta^2]$$
$$\times\exp\{-2\eta\tan^{-1}[b'/\eta(2t+1)]\}\,, \quad (2.25)$$

with

$$b'=\frac{a_{c'v'}\kappa_{c'v'}(\omega)}{a_{cv}} \quad (2.26)$$

and

$$\eta=\left(\frac{R_{cv}}{\hbar\omega_1+\hbar\omega_2-\hbar\omega_{cv}}\right)^{1/2}\,. \quad (2.27)$$

Thus, the three-band contribution to s-like excitonic final states may be written as

$$A_{fi}^{s,3b}=\sqrt{\Omega}(\phi_{\underline{n}}^{cv})_0^*\left(-\sum_{v'\neq v}\frac{\hat{\epsilon}_2\vec{p}_{cv'}(0)\hat{\epsilon}_1\cdot\vec{p}_{v'v}(0)}{\omega_{cv'}-\omega_2}I_{s,\underline{n}}(\kappa_{cv'}(\omega_2))+\sum_{c'\neq c}\frac{\hat{\epsilon}_1\cdot\vec{p}_{cc'}(0)\hat{\epsilon}_2\cdot\vec{p}_{c'v}(0)}{\omega_{c'v}-\omega_2}I_{s,\underline{n}}(\kappa_{c'v}(\omega_2))\right.$$
$$\left.+(\hat{\epsilon}_1,\omega_1\leftrightarrow\hat{\epsilon}_2,\omega_2)\right)\,, \quad (2.28)$$

where the integral $I_{s,\underline{n}}$ is given by Eqs. (2.23) and (2.25) for the bound and continuum final states, respectively. For $\kappa\ll 1$, the integral $I_{s,\underline{n}}$ can be replaced by 1. As a result, one is justified in replacing the summation (2.16) by (2.17). However, the deviation of the result (2.28) from the corresponding result for the bound excitonic states obtained by Loudon will be rather important when either $\kappa_{c'v'}(\omega_1)$ or $\kappa_{c'v'}(\omega_2)$ is comparable to unity. This corresponds to $\hbar\omega_1$ or $\hbar\omega_2$ approaching the 1s excitonic level of the bands $c'v'$, i.e., a resonance in the intermediate state. Such a situation may be encountered when we study two-photon transitions from deeper valence bands or to higher conduction bands. As an illustration, let us consider $\hbar\omega_2$ approaching the 1s intermediate exciton energy $\hbar\omega_{c'v'}-R_{c'v'}$. Loudon's approximate calculation, as well as our complete calculation, predicts a resonance enhancement; only the resonant term needs to be considered in Eq. (2.28). The ratio $\Delta\alpha^{(2)}/\Delta\alpha^{(2)}_{\text{Loudon}}$ of the enhancements depicted by the exact and the approximate expressions is given by $|I_{s,\underline{n}}(\kappa_{c'v'}(\omega_2))|^2$ and differs significantly from 1. We show this for the 1s excitonic *final* state in Fig. 1 for $\mu_{cv}=\mu_{c'v'}$. Our calculations also show that in many cases of interest, excitonic effects in the intermediate state may produce corrections of about 20% for $\hbar(\omega_{c'v'}-\omega_1)$, $\hbar(\omega_{c'v'}-\omega_2)\lesssim 10R_{c'v'}$.

The two-band contribution to s excitonic final states was calculated by Mahan.[4] His result can be written as[14]

$$A_{fi}^{s,2b}=+\tfrac{4}{3}\sqrt{\Omega}(\phi_{\underline{n}}^{cv})_0^*\,m\hbar(\hat{\epsilon}_2\cdot M_{cv}\cdot\hat{\epsilon}_1)$$
$$\times J_{s,\underline{n}}(\kappa_{cv}(\omega_2))+(\hat{\epsilon}_1,\omega_1\leftrightarrow\hat{\epsilon}_2,\omega_2)\,, \quad (2.29)$$

where the integral $J_{s,\underline{n}}(\kappa)$ is given by Eqs. (3.24) and (3.27) of Ref. 4 for the bound and continuum final states, respectively. For $\kappa\ll 1$, $J_{s,\underline{n}}(\kappa)\simeq\kappa$. When the two frequencies ω_1 and ω_2 are comparable and are away from all interband resonances, the two-band term is smaller than the three-band term by a factor κ_{cv} and has nearly the same spectral dependence. Also, the polarization dependence of the two terms is similar. It should be emphasized, however, that the two contributions (2.28) and (2.29) and their ratios are sensitive to the frequencies ω_1 and ω_2. When the two contributions are comparable, their relative sign is of great importance because one has to add the two amplitudes algebraically. To illustrate this point, let us consider the situation in which one of the two frequencies, say ω_1, is very small compared to the other (ω_2). Further, let us assume that the intermediate bands involved in the three-band term are either much above the final conduction band c or much below the final valence band v. In other words, $\kappa_{c'v'}(\omega_1)$ and $\kappa_{c'v'}(\omega_2)$ are much smaller than one.

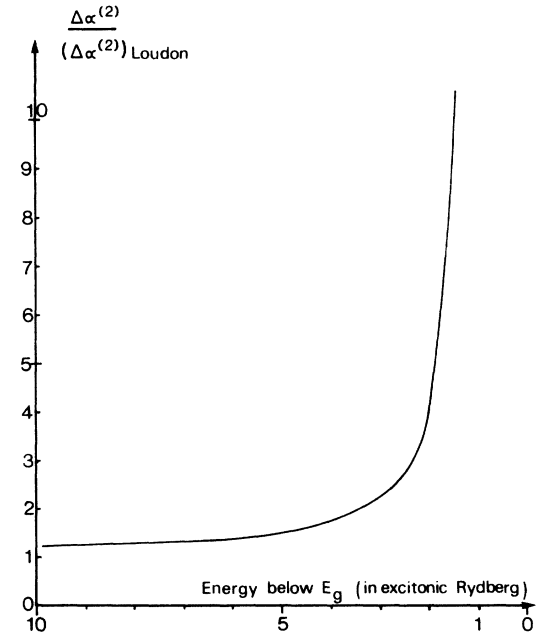

FIG. 1. Effect of excitonic intermediate state in the three-band model (see text).

The integrals $I_{s,\underline{n}}(\kappa)$ may be approximated by unity. Using Eqs. (2.13) and (2.28) in this approximation we find

$$A_{fi}^{s\,3b} \simeq -m\hbar\sqrt{\Omega}(\phi_{\underline{n}}^{cv})_0^*(\hat{\epsilon}_2 \cdot M_{cv} \cdot \hat{\epsilon}_1) \,. \qquad (2.30)$$

The next-higher-order terms in (2.30) are smaller by a factor ω_1/ω_2 or $\kappa_{c'v'}(\omega_2)$. To the same approximation as that for (2.30) the two-band term simplifies to

$$A_{fi}^{s\,2b} \simeq \tfrac{4}{3} m\hbar\sqrt{\Omega}(\phi_{\underline{n}}^{cv})_0^*(\hat{\epsilon}_2 \cdot M_{cv} \cdot \hat{\epsilon}_1) J_{s,\underline{n}}(\kappa_{cv}(\omega_2)) \,. \qquad (2.31)$$

We note that $\kappa_{cv}(\omega_2) = [R_{cv}/(\hbar\omega_{cv} - \hbar\omega_2)]^{1/2}$ must in any case be less than 2, in order that the integral representation [see Eq. (3.8) of Ref. 4] of $W_{\kappa,3/2}$ used in the theoretical analysis[4] be convergent. The limit value $\kappa(\omega_2) = 2$ corresponds to a resonance in the intermediate state, because $\hbar\omega_2$ equals $\hbar\omega_{cv} - \frac{1}{4}R_{cv}$, the energy of the $2p$ exciton. Thus, as $\hbar\omega_2$ approaches the $2p$ excitonic energy, $J_{s,\underline{n}}(\kappa_{cv}(\omega_2))$ attains larger and larger values and the two-band contribution may become larger than the three-band contribution. The $1s$ final state is, however, an interesting exception. In this case, the upper limit for $\hbar\omega_2$ is $\hbar\omega_{cv} - R_{cv}$, which corresponds to $\omega_1 = 0$, $\kappa_{cv}(\omega_2) = 1$, and $J_{s,1}(\kappa = 1) = \frac{3}{4}$. Thus, in this situation the two-band contribution annuls the three-band one. Due to this cancellation, we expect that the relative oscillator strength of $1s$ excitonic lines may be considerably lower than that expected either on the basis of a two-band model or a three-band model alone. On the basis of Eqs. (2.1), (2.30), and (2.31) we also predict that the TPA to s-excitonic levels ($\underline{n} \geq 2$) will increase sharply as we make one of the two frequencies (ω_1, in the above discussion) smaller and smaller. Such an increase is proportional to M_{cv}, which is a measure of the k dependence of $p_{c,v}(\vec{k})$. M_{cv} vanishes if c and v are both localized states.[12]

p-Excitonic Final States

Following the same methods as those above, the three-band contribution to p-excitonic final states can be written as

$$A_{fi}^{p\,3b} = \sqrt{\Omega}\left\{-\sum_{v' \neq v}\left[\frac{\hat{\epsilon}_1 \cdot \vec{p}_{v'v}(0)\hat{\epsilon}_2 \cdot M_{cv'} \cdot (\vec{p}\,\phi_{\underline{n}}^{cv})_0^*}{\omega_{cv'} - \omega_2} I_{1,\underline{n}}(\kappa_{cv'}(\omega_2)) + \frac{\hat{\epsilon}_1 \cdot M_{v'v} \cdot (\vec{p}\,\phi_{\underline{n}}^{cv})_0^* \hat{\epsilon}_2 \cdot \vec{p}_{cv'}(0)}{\omega_{cv'} - \omega_2} I_{2,\underline{n}}(\kappa_{cv'}(\omega_2))\right]\right.$$

$$\left. + \sum_{c' \neq c}\left[\frac{\hat{\epsilon}_1 \cdot \vec{p}_{cc'}(0)\hat{\epsilon}_2 \cdot M_{c'v}(\vec{p}\,\phi_{\underline{n}}^{cv})_0^*}{\omega_{c'v} - \omega_2} I_{1,\underline{n}}(\kappa_{c'v}(\omega_2)) + \frac{\hat{\epsilon}_1 \cdot M_{cc'}(\vec{p}\,\phi_{\underline{n}}^{cv})_0^* \hat{\epsilon}_2 \cdot \vec{p}_{c'v}(0)}{\omega_{c'v} - \omega_2} I_{2,\underline{n}}(\kappa_{c'v}(\omega_2))\right]\right\}$$

$$+ (\epsilon_1, \omega_1 \leftrightarrow \epsilon_2, \omega_2) \,, \qquad (2.32)$$

where for bound final states the integrals I_1 and I_2 are given by

$$I_{1,\underline{n}}(\kappa) = \int_0^\infty dt\, t^{1-\kappa}(1+t)^{1+\kappa}\left[\frac{(t+\frac{1}{2}-1/2b)^{\underline{n}-3}(t+\frac{1}{2}-\underline{n}/4b)}{(t+\frac{1}{2}+1/2b)^{\underline{n}+3}}\right] \qquad (2.33)$$

and

$$I_{2,\underline{n}}(\kappa) = \int_0^\infty dt\left(\frac{1+t}{t}\right)^\kappa (t+\tfrac{1}{2})\frac{(t+\frac{1}{2}-1/2b)^{\underline{n}-2}}{(t+\frac{1}{2}+1/2b)^{\underline{n}+2}} \qquad (2.34)$$

The integrals for the continuum final states are obtained by changing $\underline{n} \to -i\eta$ as in all previous cases. As for $A_{fi}^{s\,3b}$, the two square brackets in Eq. (2.32) correspond to the valence- and conduction-band intermediate states, respectively. In each square bracket there are two terms. The first of these corresponds to the formation of a p exciton in the intermediate state, the interexcitonic transition then takes place between two p excitons. The second term corresponds to the formation of an s exciton in the intermediate state. In this case, the interexcitonic transition takes place from the s to p excitonic levels. We notice the similarity between this sequence and the two-band scheme. In fact, if we neglect the difference between the effective masses of the intermediate- and final-state excitons, the parameter b becomes n/κ and the integral $I_{2,\underline{n}}(\kappa)$ reduces to $(1/\kappa^2)J_{p,\underline{n}}(\kappa)$ [see Eq. (2.14) of Ref. 4] in the two-band term.

For comparison, we also write the two-band term leading to p excitons,

$$A_{fi}^{p\,2b} = \sqrt{\Omega}\,\frac{m\hbar}{\mu_{cv}R_{cv}}\,\hat{\epsilon}_1 \cdot \vec{p}_{cv}\hat{\epsilon}_2 \cdot (\vec{p}\,\phi_{\underline{n}}^{cv})_0$$

$$\times J_{p,\underline{n}}(\kappa_{cv}(\omega_1)) + (\hat{\epsilon}_1, \omega_1 \leftrightarrow \hat{\epsilon}_2, \omega_2) \,, \qquad (2.35)$$

where the integral $J_{p,\underline{n}}(\kappa)$ is given by Eqs. (2.14) and (2.24) of Ref. 4. For small values of κ, $J_{p,\underline{n}}(\kappa)$ may be approximated by κ^2. The relative magnitude of the two-band and the three-band terms depends on the intermediate state contributing to the three-band terms and the frequencies ω_1 and ω_2.

If the intermediate band is not near the final bands c or v, the two-band term would dominate, at least when one of the two frequencies is small. When ω_1 and ω_2 are not very different, the spectral dependence of the two terms does *not* differ substantially. The spectral dependence of the continuum p excitonic final states is, however, rather different from that of the s excitonic final states. As in the fundamental optical spectra, this happens because the absorption coefficient to p excitonic final states is proportional to $(\nabla\phi_{\underline{n}}^{cv})_0^2$, while that to the s excitonic final states is proportional to $(\phi_{\underline{n}}^{cv})_0^2$. The two-band model gives rather simple predictions for the polarization dependence. Deviation from these predictions for the polarization should be interpreted in terms of the three-band terms. For example, in cubic crystals, the two-band model predicts TPA to p excitonic final states to be independent of the orientation of the crystal axes. If experimentally, TPA depends on the crystal axes or if $\alpha^{(2)}(\hat{\epsilon}_1 \perp \hat{\epsilon}_2)/\alpha^{(2)}(\hat{\epsilon}_1 \parallel \hat{\epsilon}_2)$ is less than one half or more than one, the three-band contributions to p excitonic final states become important.[10]

III. EXPERIMENTS

The induced absorption coefficient $\alpha^{(2)}$ is given by the relation

$$\phi(\omega_2)/\phi_0(\omega_2) = e^{-\alpha^{(2)} l} ,$$

where $\phi(\omega_2)$ represents the variable frequency flux ω_2 transmitted through a sample of length l when it is illuminated by the fixed frequency flux ω_1 provided by a laser. The transmitted flux in the absence of the laser light is denoted by $\phi_0(\omega_2)$. The induced absorption coefficient $\alpha^{(2)}$ is proportional to the laser power P_1. The crystal being centrosymmetric, there is no loss of the variable frequency flux due to sum frequency generation and subsequent absorption. Processes involving absorption of more than one laser photon are also expected to be negligible, because we have $E_g > 2\hbar\omega_1$.

The experimental setup is shown schematically in Fig. 2. A Nd^{3+}-glass laser D, Q spoiled with a rotating prism A, gives a 40 nsec pulse at 9440 cm^{-1} with a maximum peak intensity $\simeq 100$ MW/cm^2. The rotating prism (frequency 400 Hz) also provides a low jitter ($< 10^{-7}$ sec) signal B which after a suitable time delay S triggers the variable frequency light source. The delay S is so adjusted that the laser pulse falls on the flat part of the flash pulse shape. The exit mirror of the laser is made of a plane parallel glass plate (E, E0046 Sovirel) of high refractive index which acts as a Fabry-Perot etalon. The outcoming light is linearly polarized by putting several glass plates C at Brewster angle in the cavity. A $\frac{1}{2}\lambda$ quartz plate G allows us to vary the polarization direction continuously. The spectral characteristics of the laser were analyzed by recording the spectrum of its second harmonic generated in a potassium dihydrate phosphate (KDP) crystal. Typically there are five longitudinal modes, 1.39 cm^{-1} apart, in the spectral width at half-intensity. The position of the modes was found to be very stable in time. The interval between the modes corresponds exactly to the mode separation of the output Fabry-Perot etalon.

The laser beam is focused in the middle of a 150-cm long cell H filled with hydrogen or methane gas at room temperature and a pressure of 10–40 bar. As a result of stimulated Raman scattering in the cell about 10% of the laser intensity is converted to the first Stokes's component. A silicon plate I (for methane) or BG18 and RG2 Schott glass

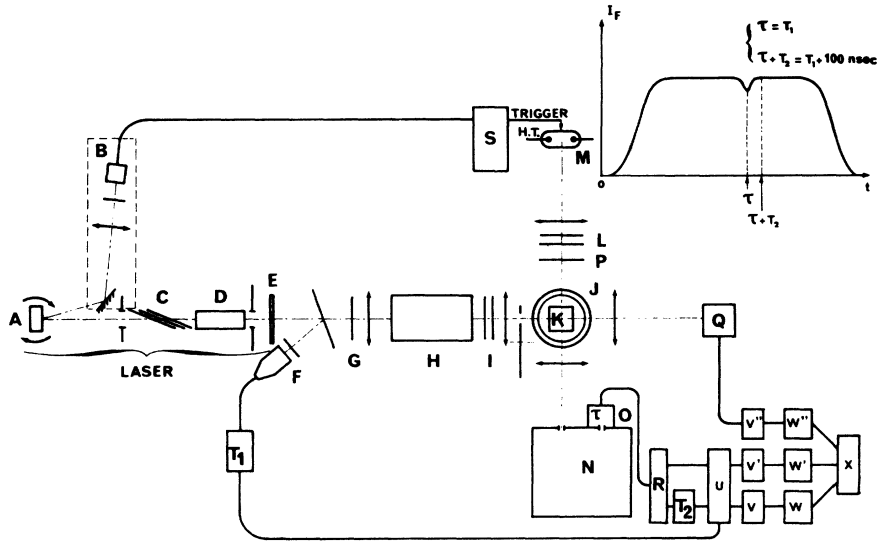

FIG. 2. Experimental setup (see text).

filters (for hydrogen) remove the primary beam while transmitting the Stokes's component at 5285 cm^{-1} for hydrogen and 6524 cm^{-1} for methane. The intensity of this component is monitored with a germanium detector Q placed after the sample. It was verified that no noticeable spectral broadening occurred during stimulated Raman scattering by analyzing the first and the second anti-Stokes's components.

The variable-frequency light beam is provided by the discharge of a capacitor band (80 μF, 2000 V) in a xenon flash tube M (GE, FT-230). This yields a smooth pulse of duration $\simeq 15$ μsec in a wide spectral range ($\lambda = 3000-15000$ Å), except in two regions, 9035–9065 Å and 8810–8840 Å, where the emission is irregular in time and prevents any reliable measurements.

In order to avoid one-photon excitation of the sample, high-energy components ($\hbar\omega_2 > 2$ eV) of the emitted light are filtered using Schott RG filters L. The light beam is linearly polarized with a plastic polaroid P placed in front of the sample. A grating monochromator (Spex 1704) N placed after the sample selects the frequency to be studied. The flux $\phi(\omega_2)$ and $\phi_0(\omega_2)$ are measured with a high-current photomultiplier O (RCA FT-4008 or Radiotechnique 56 CVP) put at the exit slit of the monochromator. It was verified that the photomultiplier always worked in its linear-response region. The data are recorded in the following manner: The output signal at the anode of the photomultiplier is divided in two identical parts, one of which is retarded by $\tau = 100$ nsec with a passive delay line. A trigger signal derived from the laser pulse and conveniently retarded to account for the transit time of the electrons in the photomultiplier initiates the electronic circuitry enabling one to measure the flux $\phi(\omega_2)$ at time t corresponding to the laser pulse falling on the sample, and the flux $\phi_0(\omega_2)$ at time $t+\tau$. The two measurements are amplified and recorded separately in channels V and V', respectively. The corresponding intensity of the laser is registered on a third channel V''. The same two measurements are alternately repeated with and without the laser pulse illuminating the sample. In this way, any differences in the gain characteristics of the channels V and V' as well as any change in the emission shape of the flashtube are minimized. Via the three digital converters W, W', W'' the data in the three channels are punched on a tape X which is analyzed by means of a computer program. Typically, 100 cycles of measurements are performed at each wavelength. This permits improvement of the signal-to-noise ratio by averaging over shot noise. The crystal is kept at 77 °K in a quartz-window Dewar K.

The cuprous-oxide single crystal used was 0.3 $\times$ 0.3 $\times$ 0.6 cm in size. It is grown by the arc-image furnace technique. An x-ray diffraction analysis revealed that the crystal axes in neighboring regions could differ by very small angles (>2°). This indicates the presence of some internal strains in the crystal. However, we found that the one-photon electric quadrupolar absorption to the 1s exciton level of the yellow series is not broadened by these internal strains. The measured width at half-maximum absorption is 1.3 cm^{-1}, which assures us of the good quality of this crystal.

The frequency region $1.4 < \hbar\omega_2 < 1.8$ eV could not be studied in our sample because of the occurrence, at 77 °K, of a broad emission band in this frequency range. This band appeared whenever the sample was illuminated by the laser beam. The emission intensity was found to be proportional to the third power of the laser intensity. Thus, it was found difficult to obtain reliable results for two-photon transitions to the higher-energy excitons of the yellow series and the green series. The energy range $\hbar\omega_1 + \hbar\omega_2 < 2.5$ eV could not be studied with another value of $\hbar\omega_1$ because then $\hbar\omega_2$ would lie in the infrared where detection is considerably less sensitive.

IV. RESULTS AND DISCUSSION

Cu_2O belongs to the O_h group. The fact that there is a center of inversion leads to a simplification in the interpretation of the results, because it is possible to neglect sum-frequency generation processes. As it has been recognized recently,[15–18] this is not the case for noncentrosymmetric crystals, where effects arising from the second-order nonlinear susceptibility may contribute significantly to the attenuation of the light beams. The linear optical properties of cuprous oxide have been extensively studied.[2] A widely accepted band scheme, first proposed by Elliott,[19] is represented in Fig. 3. All bands are parabolic with extrema at the center of the Brillouin zone. The wave functions of the highest valence bands v_1 and v_2 at $\vec{k} = 0$ transform like the Γ_7^+ and Γ_8^+ irreducible representations of the point group O_h.[20] Those of the conduction bands c_1 and c_2 transform like Γ_6^+ and Γ_7^- representations, respectively. In the tight-binding approximation, the top ten valence bands are expected to be formed from the 2p orbitals of O and 3d orbitals of Cu ions. Of these, only one has a negative parity. This band v' of symmetry Γ_4^- at $\vec{k} = 0$ (Γ_8^- and Γ_6^- with spin-orbit interaction) is formed from the 2p orbitals of O. An augmented-plane-wave (APW) band-structure calculation[21] indicates that v' is about 5.6 eV below the highest valence band v_1.

The lowest band edge ($\Gamma_7^+ \rightarrow \Gamma_6^+$) occurs at an energy of 2.1 eV. The two-photon absorption spectrum measured at 77 °K with $\hbar\omega_1 = 0.655$ eV and $1.35 < \hbar\omega_2 < 1.45$ eV, is shown in Fig. 4. In this

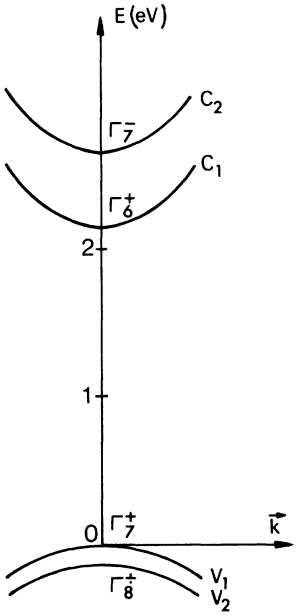

FIG. 3. Band scheme of Cu_2O near the center of the Brillouin zone (after Elliott, Ref. 19). The irreducible representation characterizing the various bands at $\vec{k}=0$ is indicated in the notation of Koster *et al.* (Ref. 20).

experiment, the laser beam was polarized along a ⟨100⟩ axis of the crystal. The flash beam was not polarized since a loss in the intensity of the flash beam would further deteriorate the poor signal-to-noise ratio. As shown in Fig. 4, a peak is observed at $\hbar(\omega_1+\omega_2)=2.025$ eV. Its position corresponds to that of the $n=1$ quadrupole line of the yellow series. Due to the rather poor resolution of the detection in the infrared, the observed width of the line is, however, larger by a factor of 60 than the corresponding quadrupole line, as measured in the same sample (see Fig. 5). Accordingly, with improved resolution, a considerable increase in the peak absorption should occur. The two possible symmetries for the excitons with s-like envelope function and formed from the bands c_1 and v_1 are Γ_2^+ and Γ_5^+. Of these, only the Γ_5^+ state can be created in a two-photon electric dipole, as well as one-photon electric quadrupole transition. In the chosen experimental configuration, the strength of the line is independent[22,23] of $\vec{\epsilon}_2$.

As discussed in Sec. II, a two-photon transition to an s-like excitonic state can occur through the two-band *and* the three-band terms. The evaluation of the three-band term depends on which bands act as intermediate states. These bands must be connected to c_1, as well as v_1 by the momentum operator $\vec{p}$, which transforms like the Γ_4^- irreducible representation of the O_h group. It is important to notice here that c_2 does not fulfill this condition, as can be seen from group-theoretical arguments: The product $\Gamma_6^+\times\Gamma_7^-\times\Gamma_4^-$ does not contain the identity

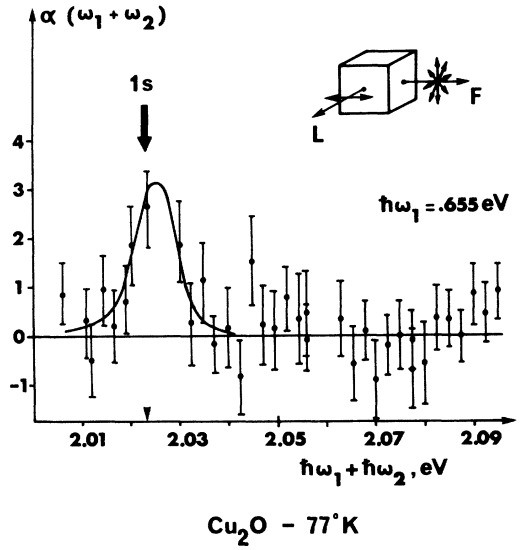

FIG. 4. Two-photon absorption spectrum of Cu_2O, at 77 °K, in the region of the $n=1$ line of the yellow excitonic series. The laser beam $\hbar\omega_1=0.655$ eV has its polarization vector $\vec{\epsilon}_1$ along a ⟨100⟩ axis, $\vec{\epsilon}_2$ is perpendicular to $\vec{\epsilon}_1$. The arrow indicates the position of the line, as observed in a quadrupole one-photon transition.

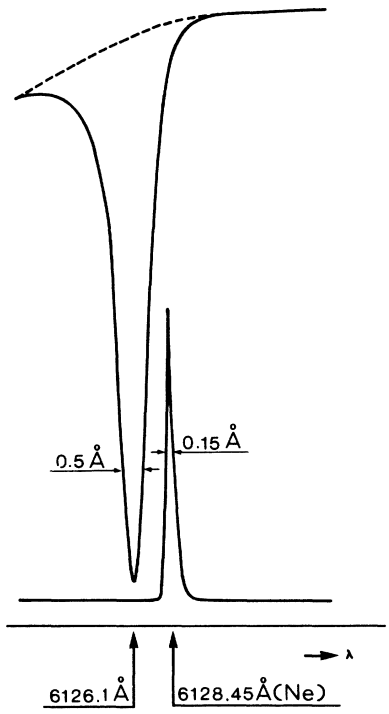

FIG. 5. One-photon absorption due to the 1s line of the yellow excitonic series of Cu_2O at 77 °K. Line 6128.45 Å, is from a neon reference lamp.

representation Γ_1^+. The nearest such band is the relatively deep (~5.6 eV) valence band v' with symmetry Γ_8^-. Due to the large energy separation of this band from c_1 and v_1, $\kappa_{c_1v'}(\omega)$ and $\kappa_{v_1v'}(\omega)$ are much smaller than 1. Thus, it is a good approximation to replace $I_{s,n}(\kappa)$ by 1. Further, it is justified to neglect ω_1 compared to $\omega_{c_1,v'}$ and $\omega_{v_1,v'}$. The three-band contribution may therefore be evaluated using Eq. (2.29). The two-band term is also known from Eq. (2.30). We find

$$\frac{A_{fi}^{s,2\text{band}}}{A_{fi}^{s,3\text{band}}} = -\frac{4}{3}\left\{J_{s,\underline{n}}(\kappa_{cv}(\omega_2)) + J_{s,\underline{n}}(\kappa_{cv}(\omega_2))\right\},$$

where we have used the fact that in this case the absorption coefficient is symmetric in $\vec{\epsilon}_1$ and $\vec{\epsilon}_2$. The values of $J_{s,\underline{n}}(\kappa_{cv}(\omega_1))$ and $J_{s,\underline{n}}(\kappa_{cv}(\omega_2))$ are 0.227 and 0.306, respectively. Thus, the two-band and the three-band contributions are comparable and of opposite sign. The net effect is that the oscillator strength of the 1s excitonic line is smaller by a factor of 12 than that calculated by Loudon on the basis of a three-band model alone. To compare our theoretical and experimental results for the discrete line, we calculate the corresponding oscillator strengths per unit cell defined as

$$f_{\underline{n}}^{(2)} = \frac{mcn_2}{2\pi^2 Ne^2}\int \alpha^{(2)}(\omega_1+\omega_2)\,d\omega_2,$$

where N is the number of unit cells per unit volume of the crystal. Using our results including both the two- and three-band terms, we find a theoretical value

$f_{1s}^{(2)} = 1.4.10^{-10}$ for a laser intensity of 3 MW/cm^2. The experimental value is

$$f_{1s}^{(2)} \simeq 10^{-10}$$

per unit cell and for the same laser intensity. This is in good agreement, in view of the lack of accuracy in the measurement of the laser intensity. As it will be shown later, the measured value of I_t leads to a good agreement between theory and experiment in other parts of the spectrum.

The TPA spectrum with $\hbar\omega_1 = 0.81$ eV and $\hbar(\omega_1+\omega_2) \geq 2.5$ eV close to the second energy gap is shown in Figs. 6 and 7 for $\vec{\epsilon}_1 \parallel \vec{\epsilon}_2$ and $\vec{\epsilon}_1 \perp \vec{\epsilon}_2$, respectively. (Results obtained in the same region on a polycrystal with $\hbar\omega_1 = 0.655$ eV have been presented earlier and are not reproduced here.[7])

The spectral range covered in Figs. 6 and 7 can be conveniently divided into three regions. Region I ($\hbar\omega_1+\hbar\omega_2 \leq 2.55$ eV) is attributed to two-photon transitions from the two valence bands v_1 and v_2 to the lowest conduction band c_1.

In region II, where $\hbar(\omega_1+\omega_2)$ is close to the 1s excitonic level of the blue series ($E = 2.548$ eV), one observes a structure, which requires some explanation, since a two-photon transition to an s

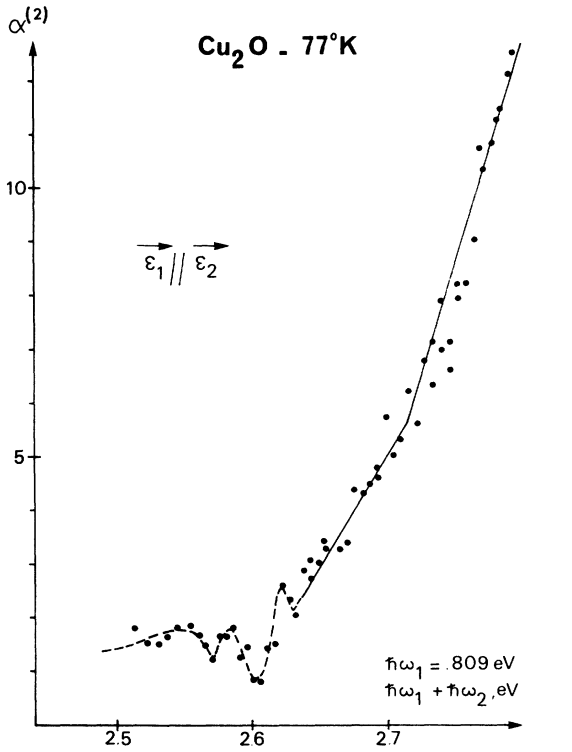

FIG. 6. Two-photon absorption spectrum of Cu_2O, at 77 °K, in the region of the blue and violet excitonic series. Both beams are polarized parallel to each other. The solid line shows the spectral dependence calculated on the basis of a two-band model.

excitonic final state with an electron and a hole in bands of opposite parity is forbidden by the parity selection rule. In order to provide such an explanation, due consideration must be given to the fact that the discrete 1s excitonic level lies on a continuum of levels associated with the lower conduction band. The discrete and the continuum levels are mixed[24] by configuration interaction, i.e., those interactions in the system, which are not included in our approximate description of the excited states. One must now consider transitions to the mixed states. A structure near the position of the discrete state can appear,[24,25] even if the transitions to the unperturbed (by configuration interaction) discrete state are not allowed. In such a situation, however, the absorption decreases below its average value in the continuum (but the absorption coefficient integrated over the entire spectral range covered by the structure must be the same as that for the unperturbed continuum). We feel that such a situation is well reproduced in Fig. 7, even though there is considerable uncertainty in the estimate of TPA, due to the "unperturbed" continuum. In other cases (see Fig. 3 of Ref. 7), a nonvanishing two-photon transition prob-

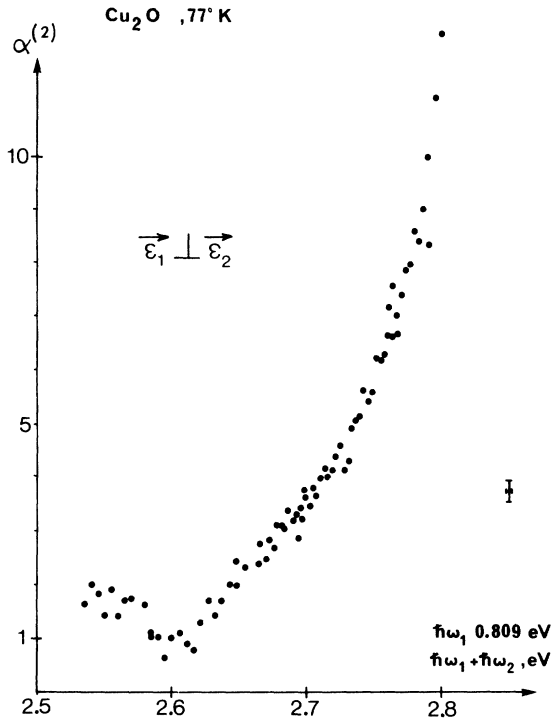

FIG. 7. Two-photon absorption spectrum of Cu_2O, at 77 °K, in the region of the blue and violet excitonic series. Both beams are polarized perpendicular to each other.

ability to the unperturbed $1s$ state of the blue series must be accounted for. One possibility for such a mechanism is provided by the presence of an inversion asymmetric perturbation in the sample, due to internal strains. This is consistent with the observation that spectra of similar Cu_2O crystals have shown some features which violate the parity selection rule.[26] For a clearer understanding of this interesting region, one needs some more measurements on different samples with an improved resolution.

The frequency region III begins as $\hbar(\omega_1+\omega_2)$ approaches the $n=2$ excitonic level of the blue series ($E=2.62$ eV). A sharp increase of $\alpha^{(2)}$ is observed for both values of ω_1 and for all polarizations studied. As discussed in Sec. II, this corresponds to the creation of p final states. We have computed $\alpha^{(2)}$ using the results of Mahan's two-band calculation.[4] The integrals $J_{pk}(\kappa)$ were evaluated using a simple computer program. The band gap and Rydberg of the blue series are taken to be 2.63 and 0.046 eV, respectively.[27] The corresponding numbers for the violet series are 2.76 and 0.047 eV. The contribution of bound p excitons was evaluated by extrapolating below the ionization limit the results for the continuum. Rather good agreement is found between the calculated and observed spectra dependence of $\alpha^{(2)}$ (see Fig. 6). The magnitude of the experimental value of $\alpha^{(2)}$ is found to be one-half the magnitude of the calculated one. We find this agreement satisfactory in view of the uncertainty associated with laser intensity measurements. The dependence of $\alpha^{(2)}$ on $\vec{\epsilon}_1$ and $\vec{\epsilon}_2$ also provides a check on the theoretical description. In the two-band model for TPA in cubic crystals with p excitonic final states, the ratio $\alpha^{(2)}(\vec{\epsilon}_1\perp\vec{\epsilon}_2)/\alpha^{(2)}(\vec{\epsilon}_1\parallel\vec{\epsilon}_2)$ is independent of the crystal axes and is given by

$$\frac{\alpha^{(2)}(\vec{\epsilon}_1\perp\vec{\epsilon}_2)}{\alpha^{(2)}(\vec{\epsilon}_1\parallel\vec{\epsilon}_2)}=\frac{J^2_{pk}(\kappa_{cv}(\omega_1))+J^2_{pk}(\kappa_{cv}(\omega_2))}{|J_{pk}(\kappa_{cv}(\omega_1))+J_{pk}(\kappa_{cv}(\omega_2))|^2}\ .$$

We measured this ratio at several frequencies, keeping all other experimental parameters constant. In Table I these results are compared with those calculated on the basis of a two-band model alone. At $\hbar(\omega_1+\omega_2)=2.78$ eV, the contribution of the violet series was also included in the calculation. The agreement between theory and experiment can be considered fair, in view of the limited accuracy of the experimental results. On the other hand, one may argue that the difference between the two sets of values indicates a contribution from the three-band term. A three-band contribution, involving the p-like excitons of the yellow and green series as intermediate states close to resonance, can be safely neglected here, because the transition between the two conduction bands c_1 and c_2 is not dipole allowed.

V. CONCLUSIONS AND SUMMARY

We have performed a detailed investigation of the two-photon absorption spectra due to excitonic states in semiconductors. The general theoretical treatment presented in Sec. II includes the excitonic effects in final, as well as intermediate states. We found it appropriate to study the s and p excitonic final states separately. As in the one-photon spectra, the spectral dependence of s- and p-like final states is different. The three-band and two-band contributions to the same kind (s or p) of excitonic final states have very similar spectral dependences except close to a resonance in the intermediate state. Away from such resonances, one expects the three-band contribution to be larger than the two-band one for s excitonic final states, while for p-like final states, the two-band contribution dominates. We also found that the Coulomb

TABLE I. Comparison between measured and calculated $\alpha^{(2)}$ (see text).

$\hbar\omega_1+\hbar\omega_2$ (eV)	$\alpha^{(2)}(\hat{\epsilon}_1\perp\hat{\epsilon}_2)/\alpha^{(2)}(\hat{\epsilon}_1\parallel\hat{\epsilon}_2)$ Calculated	Measured
2.66	0.59	0.73±0.15
2.72	0.60	0.70±0.10
2.78	0.60	0.71±0.06

effects in the intermediate state become more and more important as ω_1 or ω_2 approaches the intermediate-state energy. The dimensionless parameters $\kappa_{c'v'}(\omega_1)$ and $\kappa_{c'v'}(\omega_2)$ (c', v' are the bands in the intermediate state) provide a measure of the proximity of ω_1 and ω_2 to the intermediate-state energy. Attention is drawn to the fact that two-band and three-band terms leading to same final state can interfere destructively. This happens for the s excitonic final states. In fact, as one of the two frequencies becomes very small, the two-band and three-band terms to the 1s final state cancel each other. We should also mention that the three-band term is usually more difficult to evaluate than the two-band term because the latter involves only those parameters which are known from the one-photon spectroscopy.

Cu_2O, chosen for our experimental investigations, is well-known for excitonic effects in its optical properties. Longstanding interest in the TPA spectrum of Cu_2O is due to the fact that the smallest band gap is between bands of the same positive parity at $\vec{k}=0$. Thus, while one-photon transitions at Γ between these bands are not allowed in the electric-dipole approximation, the two-photon transitions are allowed. Further, since the second conduction band has negative parity at Γ, in this case one-photon transitions are allowed at Γ, while those involving two photons are not. Thus, while in the one-photon spectrum transitions to the second conduction band are much stronger than those to the first conduction band, the converse should be expected for the two-photon spectrum. Our experimental results show that this expectation is not fulfilled. This is essentially due to the fact that the only band which is connected to the lowest conduction band, as well as the highest two valence bands, is a deep lying valence band of symmetry Γ_8^-. The destructive interference between the two-band and the three-band terms further reduces the strength of two-photon transition to the lowest conduction band. The spectral dependence of $\alpha^{(2)}$ in the higher frequency region is well reproduced by the two-band model. The study of polarization dependence, however, indicates that the three-band terms are not negligible.

---

*Present address: Max Planck Institut für Festkörperforschung Heilbronnerstrasse, Stuttgart, Germany.

[1]A recent review of two-photon spectroscopy is given by J. M. Worlock [in *Laser Handbook*, edited by F. T. Arecchi and E. D. Schul Dubois (North-Holland, Amsterdam, 1972), Vol. 2, p. 1323]. See also, D. Fröhlich, Festkorperprobleme **10**, 227 (1970).

[2]See the review by S. Nikitine, in *Optical Properties of Solids*, edited by S. S. Mitra and S. Nudelman (Plenum, New York 1969).

[3]R. Loudon, Proc. Phys. Soc. Lond. **80**, 952 (1962).

[4]G. D. Mahan, Phys. Rev. **170**, 825 (1968).

[5]J. J. Hopfield and J. M. Worlock, Phys. Rev. **137**, A1455 (1965).

[6]See, e.g., J. M. Worlock, Ref. 1.

[7]F. Pradère, B. Sacks, and A. Mysyrowicz, Opt. Commun. **1**, 234 (1969); F. Pradère, A. Mysyrowicz, K. C. Rustagi, and D. Trivich, Phys. Rev. B **4**, 3570 (1971).

[8]R. J. Elliott, Phys. Rev. **108**, 1384 (1957); and in *Polarons and Excitons*, edited by C. G. Kuper and G. D. Whitfield (Oliver and Boyd, London, England, 1963).

[9]By $\underline{n}$ we denote all hydrogenic quantum numbers: n,l,m, for the bound state and $\vec{k}$ for the continuum states.

[10]D. Fröhlich, B. Staginnus, and Y. Onodera, Phys. Status Solidi **40**, 547 (1970).

[11]E. I. Blount, in *Solid State Physics*, edited by F. Seitz and D. Turnbull (Academic, New York, 1962), Vol. 13, p. 305.

[12]K. C. Rustagi, Solid State Commun. **12**, 607 (1973).

[13]We assume $M_{bb'} \approx 1$. For typical exciton radius ~ 10 Å and $p_{bb'} \sim 10^{-19}$ g cm^{-1} sec^{-1}, one obtains $\hbar/a\,p_{bb'} \sim 0.1$. Smallness of this parameter justifies the expansion (2.8)

[14]We find that the sign on the right-hand side of Eqs. (3.4) and (3.22) of Ref. 4 should be changed. It does not affect any conclusions of Ref. 4, but is of vital importance in our discussion. We have retained the definitions of $J_{s,n}$ as given by Eqs. (3.23) and (3.27) of Ref. 4.

[15]R. J. Elliott, Phys. Rev. **124**, 340 (1961).

[16]We use the notation of G. F. Koster, J. O. Dimmock, R. J. Wheeler, and H. Statz, *Properties of Thirty-two Point Groups* (MIT Press, Cambridge, Mass., 1963).

[17]J. P. Dahl and A. C. Switendick, J. Phys. Chem. Solids **27**, 931 (1966).

[18]E. Yablonovitch, C. Flytzanis, and N. Bloembergen, Phys. Rev. Lett. **29**, 865 (1972).

[19]D. Bogget and R. Loudon, Phys. Rev. Lett. **28**, 1051 (1972).

[20]D. Fröhlich, E. Mohler and P. Wiesner, Phys. Rev. Lett. **26**, 554 (1971).

[21]D. G. Haueisen and H. Mahr, Phys. Rev. Lett. **26**, 838 (1971); D. G. Haueisen, and H. Mahr, Phys. Lett. A **36A**, 433 (1971).

[22]M. Inoue and Y. Toyzawa, J. Phys. Soc. Jap. **20**, 363 (1965).

[23]T. R. Bader and A. Gold, Phys. Rev. **171**, 997 (1968).

[24]U. Fano, Phys. Rev. **124**, 1866 (1961).

[25]D. L. Greenaway and G. Harbeke, *Optical Properties and Band Structure of Semiconductors* (Pergamon, New York, 1968), Chap. 8.

[26]T. Reydellet, Thèse de 3ème Cycle (Université de Paris) (unpublished).

[27]The parameters for the blue and violet series are as given by S. N. Shestatskii, V. V. Sobolov, and N. P. Likhobabin, Phys. Status Solidi **42**, 699 (1970).